CANCER GENOMICS & PROTEOMICS *15*: 249-264 (2018)
doi:10.21873/cgp.20083

Effects of Sepantronium Bromide (YM-155) on the Whole Transcriptome of MDA-MB-231 Cells: Highlight on Impaired ATR/ATM Fanconi Anemia DNA Damage Response

ELIZABETH A. MAZZIO, CHARLES A. LEWIS, RASHID ELHAG and KARAM F. SOLIMAN

College of Pharmacy & Pharmaceutical Sciences, Florida A&M University, Tallahassee, FL, U.S.A.

Abstract. *Sepantronium bromide (YM-155) is believed to elicit apoptosis and mitotic arrest in tumor cells by reducing (BIRC5, survivin) mRNA. In this study, we monitored changes in survivin mRNA and protein after treating MDA-MB-231 cells with YM-155 concurrent with evaluation of whole transcriptomic (WT) mRNA and long intergenic non-coding RNA at 2 time points: 8 h sub-lethal (83 ng/mL) and 20 h at the LC_{50} (14.6 ng/mL). The data show a tight association between cell death and the precipitating loss of survivin protein and mRNA (-2.67 fold-change (FC), p<0.001) at 20 h, questioning if the decline in survivin is attributed to cell death or drug impact. The meager loss of survivin mRNA was overshadowed by enormous differential change to the WT in both magnitude and significance for over 2000 differentially up/down-regulated transcripts: (+22 FC to -12 FC, p<0.001). The data show YM-155 to up-regulate transcripts in control of circadian rhythm (NOCT, PER, BHLHe40, NFIL3), tumor suppression (SIK1, FOSB), histone methylation (KDM6B) and negative feedback of NF-kappa B signaling (TNFAIP3). Down-regulated transcripts by YM-155 include glucuronidase (GUSBP3), numerous micro-RNAs, DNA damage repair elements (CENPI, POLQ, RAD54B) and the most affected system was the ataxia-telangiectasia mutated (ATM)/Fanconi anemia E3 monoubiquitin ligase core complexes (FANC transcripts - A/B/E/F/G/M), FANC2, FANCI, BRCA1, BRCA2, RAD51, PALB2 gene and ATR (ATM- and Rad3-Related) pathway. In conclusion, these findings suggest that a primary target of YM-155 is the loss of replicative DNA repair systems.*

The data discussed in this publication have been deposited in NCBI's Gene Expression Omnibus and are accessible through GEO Series accession number GSE103089 at https://www.ncbi.nlm.nih.gov/geo/query/acc.cgi?acc=GSE103089.

Correspondence to: Karam F.A. Soliman, Ph.D., Professor & RCMI Program Director, College of Pharmacy & Pharmaceutical Sciences, Florida A&M University, Room 104 Dyson Pharmacy Building, 1520 ML King Blvd, Tallahassee, FL 32307, U.S.A. Tel: +1 850 599 3306, Fax: +1 850 599 3667, e-mail: karam.soliman@famu.edu

Key Words: Sepantronium bromide, transcriptome, Fanconi anemia, YM-155.

Breast cancer is one of the most common malignancies in females worldwide. Survivin (encoded by the BIRC5 gene) is classified as an inhibitor of apoptosis protein (IAP) which is overexpressed in various malignancies (1-5), when compared to adjacent non-cancerous tissue (6, 7). Overexpression of survivin correlates to lack of tumor senescence and unbridled mitosis as a result of binding to the inner centromere protein (ICP), aurora B kinase and borealin to form the chromosomal passenger complex (CPC), required for prophase and metaphase events (8, 9). The overexpression of survivin in malignant breast cancer models is associated with aggressive tumor growth, poor disease-free survival period, greater relapse (10, 11) and taxane-based chemotherapeutic resistance, suggesting its role in triple negative breast cancers (TNBC) could be pivotal (12). Briefly, TNBCs are a sub-type of breast cancer characterized by the absence of estrogen and progesterone receptors and HER2/neu. This type of breast cancer has an overall poor prognosis worsened by the non-feasibility of hormone receptor-based treatment options, rendering the reliance on taxane-based chemotherapies.

One of the original survivin inhibitors identified was sepantronium bromide (YM-155), a first-in-class mRNA BIRC5 inhibitor showing therapeutic potential to antagonize tumor growth, induce apoptosis and decrease mitotic indices (13). The broad and potent anti-tumor activity of YM-155 has been reported against a wide variety of human cancer cell lines and xenograft models (14) where many cell lines have been found to be exquisitely sensitive to its lethal effects in the nM range, including TNBCs (15). Previous studies evaluating the effects of YM-155 in tumor models demonstrate capacity to halt cell proliferation, reverse chemo-resistance of statin based drugs (16) and *in vivo*

establish the regression of subcutaneously implanted tumors including the MDA-MB-231 cell line in an orthotopic model (14). Agents that suppress survivin protein levels or knock out the gene appear to induce similar effects in both slowing tumor growth and providing greater sensitization to drugs such as gemcitabine (17-20) .

Although YM-155 has been described as one of the first survivin antagonists, its molecular mechanism still remains obscure. Moreover, there is a lack of public database microarray deposition for this compound in tumor models, which would define off target effects of this drug. In this study, we evaluate the effects of YM-155 on the entire transcriptome of MDA-MB-231 cells using Affymetrix WT human 2.1 ST Arrays. The data discussed in this publication have been deposited in NCBI's Gene Expression Omnibus and are accessible through GEO Series accession number GSE103089 for public analysis.

Materials and Methods

Hanks Balanced Salt Solution, 96 well plates, pipette tips, general reagents and supplies were all purchased from Sigma-Aldrich Co. (St. Louis, MO, USA) and VWR International (Radnor, PA, USA). Triple-negative human breast (MDA-MB-231) cells were obtained from American Type Culture Collection (Rockville, MD, USA). Dulbecco's modified Eagle's medium (DMEM), fetal bovine serum (FBS) and penicillin/streptomycin were obtained from Invitrogen (Carlsbad, CA, USA). All microarray equipment, reagents and materials were purchased from Affymetrix/ Thermo Fisher (Waltham, MA, USA).

Cell culture. MDA-MB-231 cells were cultured in 75 cm^2 flasks containing DMEM supplemented with 10% FBS and 1% 10,000 U/mL penicillin G sodium/10,000 μg/mL streptomycin sulfate. Cells were grown at 37˚C with 95% atmosphere/ 5% CO_2 and sub-cultured every three to five days. YM-155 was dissolved in DMSO [20 mg/mL], and dilutions were prepared in sterile HBSS, ensuring solvent concentration of DMSO or absolute ethanol at less than 0.5%.

Cell viability assay. Alamar Blue cell viability assay was used to determine cytotoxicity. Viable cells reduce resazurin to resorufin, a fluorescence product. Briefly, 96-well plates were seeded with MDA-MB-231 cells at a density of 5×10^6 cells/mL. Cells were treated with or without YM-155 for 24 h at 37˚C, 5% CO_2. Alamar Blue (0.1 mg/mL in HBSS) was added at 15% v/v to each well and the plates were incubated for 6-8 h. Quantitative analysis of dye conversion was measured using a Synergy™ HTX Multi-Mode microplate reader (BioTek, Winooski, VT, USA), at 550 nm/580 nm (excitation/emission). The data were expressed as viability: percentage of untreated controls.

Survivin protein expression. Human survivin ELISA: After treatment, cells were washed, lysed and evaluated for intracellular survivin protein expression using a survivin human SimpleStep ELISA® Kit #ab183361 (Abcam, Cambridge, MA, USA) carried out in accordance with the manufacturer's protocols. The data was quantified at 450 nm using a Synergy HTX multi-mode reader from Bio-Tek (Winooski, VT, USA).

Microarray WT 2.1 human datasets. After treatment, cells were washed three times in ice cold HBSS, rapidly frozen and stored at −80˚C. Total RNA was isolated and purified using the TRIzol/chloroform method, quality was assessed and concentration was equalized to 82 ng/μL in nuclease free water. Whole transcriptome analysis was conducted according to the GeneChipTM WT PLUS Reagent Manual for Whole Transcript (WT) Expression Arrays. Briefly, RNA was synthesized to first strand cDNA, second-strand cDNA and followed by transcription to cRNA. cRNA was purified and assessed for yield, prior to 2nd cycle single stranded cDNA synthesis, hydrolysis of RNA and purification of 2nd cycle single stranded cDNA. cDNA was then quantified for yield and equalized to 176 ng/mL. Subsequently, cDNA was fragmented, labeled and hybridized on to the arrays prior to being subject to fluidics and imaging using the Gene Atlas (Affymetrix, ThermoFisher Scientific). The array data quality control and initial processing from CEL to CHP files were conducted using expression console, prior to data evaluation using the Affymetrix transcriptome analysis console. Samples were run in triplicates (n=3). Supportive analysis was accomplished using geneontology.org (21). The data discussed in this publication have been deposited in NCBI's Gene Expression Omnibus and are accessible through GEO Series accession number GSE103089 located at https://www.ncbi.nlm.nih.gov/geo/query/acc.cgi?acc=GSE103089.

Data analysis. Statistical analysis was performed using Graph Pad Prism (version 3.0; Graph Pad Software Inc. San Diego, CA, USA) with significance of difference between the groups assessed using a one-way ANOVA and then followed by Tukey *post hoc* means comparison test, or a Student's *t*-test. LC_{50} values were determined by regression analysis using Origin Software (Origin Lab, Northampton, MA, USA).

Results

The potent cytotoxic effects of YM-155 on MDA-MB-231 cells at 24 h were originally identified from a high-throughput (HTP) toxicity screening routinely conducted at our facility on thousands of compounds. HTP screenings involving tumor cell lines are always run in tandem with both positive and negative controls which are comprised of a large panel of reference chemotherapy drugs. For the sake of brevity, we provide data on a select few chemotherapy drugs *vs*. YM-155 (Figure 1), where YM-155 was more potent than doxorubicin, irinotecan, camptothecin and staurosporine in establishing lethality in MDA-MB-231 cells. Many of these screenings are conducted in a pilot manner to serve as a rationale for in depth investigation as in the case of YM-155.

In the next series of studies, we evaluated the loss of cell viability tantamount to the loss of survivin protein content. The LC_{50} of YM-155 on MDA-MBA-231 cells was 14.6 ng/mL (32 nM) (Figure 2). Somatic survivin was first calculated using a standard curve, where the average survivin cell concentration was found to be 1177 pg/mL equating to 117.7 pg/50,000 cells (Figure 3A). Subsequently, YM-155 was capable of reducing survivin protein expression with an IC_{50}=2.1 ng/mL (Figure 3B). Given the slight drop in

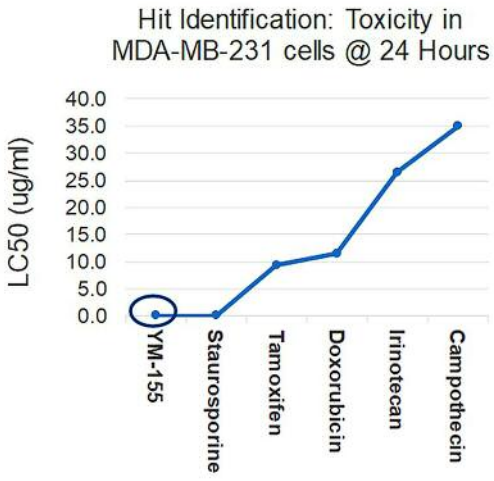

Compound	LC50 ug/ml
YM-155	0.015
Staurosporine	0.068
Tamoxifen	9.384
Doxorubicin	11.512
Irinotecan	26.421
Campothecin	34.884

Figure 1. *Lead Hit Identification: A pilot screening of over 1,000 natural products, chemicals and drugs were evaluated for lethality in MDA-MB-231 cells at a 24-h time point. The data represent effects of sample reference chemotherapy drugs used in the screen, reflected by LC_{50} calculated by dose response data acquired on a minimum of 6 concentrations, n=4. The most lethal compound at the lowest dose over 24 h was YM-155, a survivin inhibitor. These findings are in alignment with the literature.*

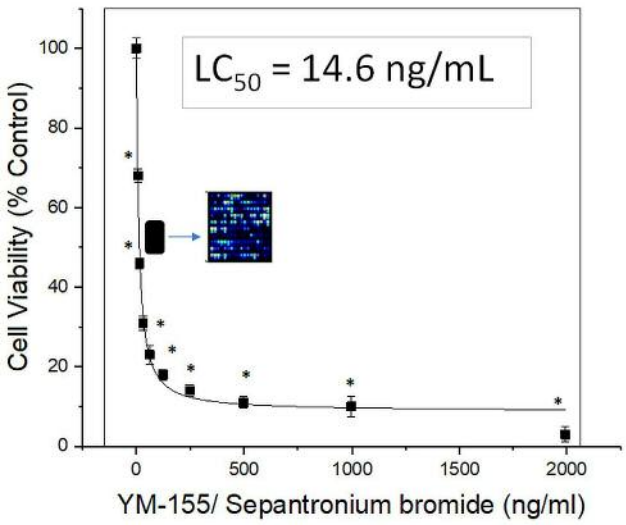

Figure 2. *YM-155 toxicity in MDA-MB-231 cells at 24 h. The data represent cell viability as % of untreated controls and are expressed as the Mean± S.E.M, n=4. Significant of differences from the control were evaluated using a one-way ANOVA, followed by a Tukey-Post Hoc Test, *p<0.05. The LC_{50} of 14.6 ng/mL is equivalent to 32 nM. ■= Concentration used for WT microarray evaluation.*

survivin, which preceded the loss in cell viability, the theoretical question arises as to if the drop in survivin could be a consequence of cell death, rather than a precipitating factor. Often time's events occur that align with cell death, that may not itself be a factor to biological provocation. To further investigate this aspect, the study was repeated in another TNBC cell line: the MDA-MB-468 cell line. The data acquired on the MDA-MB-468 cell line was even less remarkable, showing the IC_{50} for survivin at 16.9 ng/mL corresponding to loss of viability with an LC_{50} at 34.35 ng/mL (data not shown). The loss of survivin in both cases was only observed at concentrations slightly preceding cell death. To further investigate if meager changes in the survivin protein by YM-155 were reflected at the genomic level, samples were analyzed for changes to the whole transcriptome (WT) by genomics microarray methodology.

RNA was collected from cells treated with 14.6 ng/mL of YM-155 at 20 hours, where the data show a meager reduction in survivin (-2.7 FC, $p<0.001$). The change in survivin was largely overshadowed by changes in 2,592 transcripts, many of which had greater FC and significance (Figure 4). Given that cell death alone may constitute an interfering variable to WT data, a second WT data set was obtained at an earlier time point (8 hours) where death had not occurred yet, and concentrations were adjusted for sub-lethal/high concentration (83 ng/mL) (Figure 5). This concentration was high enough to trigger what would be a complete loss of cell viability at 24 hours, suitable for examining events precipitating at the cusp of cell death.

Transcriptome differentially expressed transcripts are presented for both 8 and 20-h time points in the form of a volcano plot showing FC *vs*. significance (*p*-value), from triplicates n=3 (Figure 6A and B). Figure 6A and B shows a high degree of overlap for specific transcripts at both time points, these transcripts are also being presented in Table I. Table I shows only the transcripts common to both time points, where the entire data series for control *vs*. 8 h, and control *vs*. 20 h are available at: NCBI's Gene Expression Omnibus and are accessible for public analysis through GEO Series accession number GSE103089 located at https://www.ncbi.nlm.nih.gov/geo/query/acc.cgi?acc=GSE103089 Again, these findings clearly show a plethora of changes occurring tantamount to the loss of the survivin transcript, suggesting this is unequivocally not a single target drug.

The spot intensity bi-weighted average signal (log2) for survivin quantified on all 9 oligonucleotide arrays is presented

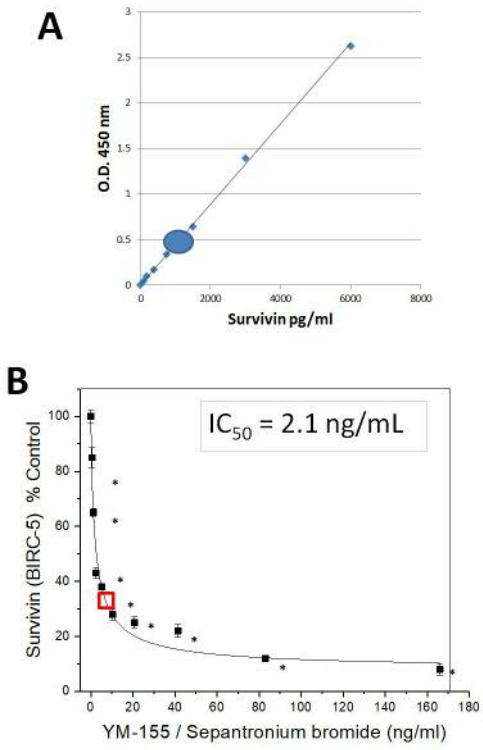

Figure 3. *(A) ELISA standard curve for human survivin. ● denotes the average expression of survivin in untreated MDA-MB-231 cells=1,177 pg/mL equating to 117.7 pg/50,000 cells prepped in 100ul of lysate buffer. (B) Intracellular concentration of survivin in YM-155 treated MDA-MB-231 cells at 24 h. The data represents survivin concentration as % of untreated controls and are expressed as the Mean±S.E.M, n=3. Significance of differences from the control were evaluated using a one-way ANOVA, followed by a Tukey-Post Hoc Test, *p<0.05.*

in Figure 7. Figure 7 shows reduction of BIRC5 as a minor shift relative to the vast predominating effects of YM-155 which by 20 h had significant impact on the following processes: DNA replication (Figure 8), DNA damage (Figure 9), cell cycle (Figure 10) and apoptosis (Figure 11). Down-regulated transcripts are denoted by solid red, up-regulated transcripts by solid green, and ///// = no statistical differences.

These findings show major changes by YM-155 to invoke major loss to the efficacy of normal DNA damage response, which is likely to be a formidable and primary mechanism of action for this drug.

Discussion

Survivin is an inhibitor-of-apoptosis protein with key roles in driving uncontrolled cell division in aggressive malignancies. Small-molecule survivin inhibitors are a

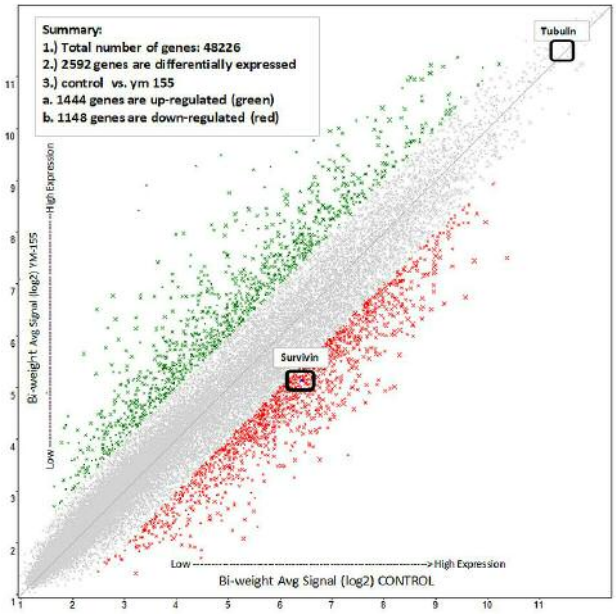

Figure 4. *Whole transcriptome differential shift by YM-155 (14.6 ng/mL) in MDA-MB-231 cells at 20 h, criteria set at: FC +/-2, p-Value<0.05. The data is presented as Bi-weighted Ave Signal (Log2) of raw intensity values, with expression (low) to (high) and distance from the central diagonal line being FC down (red) or up (green). Amidst the differentially expressed genes is □ the survivin transcript, -2.67 FC, ANOVA p-Value=0.0000907, n=3.*

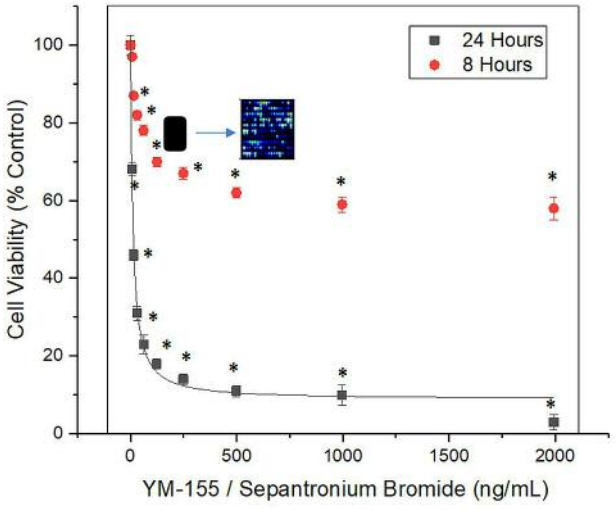

Figure 5. *Sub-lethal YM-155 concentration setup for WT microarray. Optimum concentration was 83 ng/mL which at 8 h showed little effects on viability, but was high enough to trigger complete cell death over the next 16 h. The data represents cell viability as % untreated controls and are expressed as the Mean±S.E.M, n=4. Significance of differences from the control values were evaluated using a one-way ANOVA, followed by a Tukey-Post Hoc Test, *p<0.05. ■= Concentration used for WT microarray evaluation.*

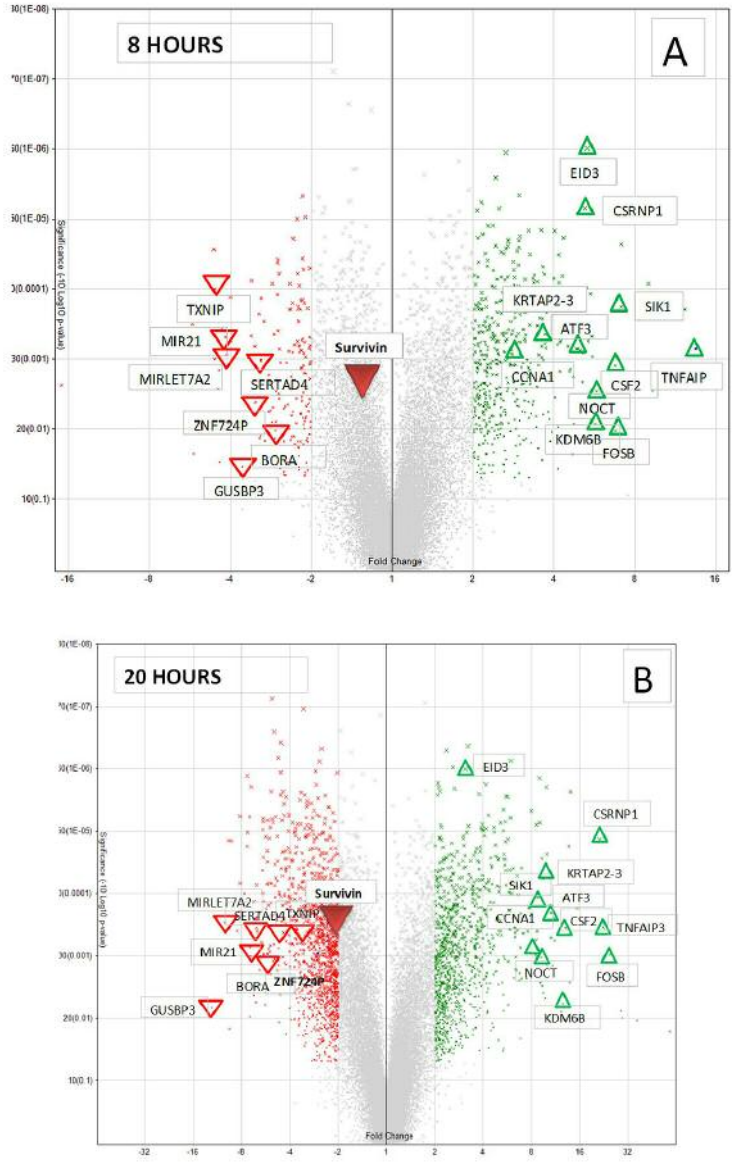

Figure 6. *(A, B) Time-dependent effects on transcripts of YM-155-treated MDA-MB-231 cells: (A) for 8 h (83 ng/mL) (B) for 20 h (14.6 ng/mL). The data are plotted as a volcano, showing both FC (X-Axis) <2x - (negative)/red and - >2x (positive)/green and significance on the Y-Axis, n=3. Highlighted changes for specific genes describe those altered at both time points. These are likely to be most influential in YM-155 mediated toxicological effects.*

sought after chemotherapy drug classification, to which sepantronium bromide (YM-155) is believe to be best in in class. (22-24) YM-155 has been reported to overcome drug resistance (*e.g.* statins (16, 25-27) docetaxel (28)), improve efficacy of diverse therapies including hypericin-mediated photodynamic therapies (29) and on its own merit, induces apoptosis, reduces colony formation, attenuates invasion and growth of xenograft tumors in nude mice (30-33). While reduction of survivin by YM-155 is believed to be a foremost mechanism of action, other biochemical targets for this drug are continually being reported in the literature. Just for example, YM-155 has been reported to alter transcription of FOS, JUN and c-MYC (34), pro-apoptotic Bak (35), p53 (22), death receptor 5, other IAP family member proteins (BIRC2, MCL-1), PI3K-Akt (31) and autophagy regulating components such as Beclin1 (36-38). In this study, we provide supportive information as to the diverse transcriptome targets of YM-155 in TNBC cells while maintaining a benchmark differential comparative in survivin protein and mRNA changes.

Table I. *The data represent Gene Symbol, description, cluster ID, Fold-Change, ANOVA p-value and FDR p-values.*

Up-regulated by YM-155			8-hour			20-hour		
Gene Symbol	Description	Cluster ID	**FC at 8 h**	ANOVA *p*-value	FDR *p*-value	**FC at 20 h**	ANOVA *p*-value	**FDR *p*-value**
FOSB	FBJ murine osteosarcoma viral oncogene hom B	16863287	**6.8**	0.011	0.157	**24.7**	0.001	**0.021**
TNFAIP3	Tumor necrosis factor, alpha-induced protein 3	17012946	**13.5**	0.001	0.048	**22.3**	<0.001	**0.013**
CSF2	Colony stimulating factor 2	16988971	**6.8**	0.001	0.058	**13.0**	<0.001	**0.014**
ATF3	Activating transcription factor 3	16677278	**5.4**	0.001	0.044	**10.6**	<0.001	**0.011**
KRTAP2-3	Keratin associated protein 2-3	16844585	**3.7**	0.001	0.045	**9.4**	<0.001	**0.006**
RNVU1-14	RNA, variant U1 small nuclear 14	16670212	**3.6**	0.027	0.252	**9.4**	0.004	**0.045**
KDM6B	Lysine (K)-specific demethylase 6B	16830754	**5.7**	0.008	0.142	**9.3**	0.003	**0.039**
NOCT	Nocturnin	16970853	**5.8**	0.003	0.085	**9.2**	0.001	**0.023**
CSRNP1	Cysteine-serine-rich nuclear protein 1	16952414	**4.3**	<0.001	0.020	**9.0**	<0.001	**0.003**
SIK1	Salt-inducible kinase 1	16926200	**7.1**	<0.001	0.028	**8.7**	<0.001	**0.008**
CXCL8	Chemokine (C-X-C motif) ligand 8	16967771	**5.1**	0.002	0.073	**8.6**	0.001	**0.017**
CCNA1	Cyclin A1	16774053	**2.6**	0.004	0.095	**8.0**	<0.001	**0.011**
HMGCS1	3-hydroxy-3-methylglutaryl-CoA synthase 1	16995890	**3.0**	<0.001	0.020	**8.0**	<0.001	**0.004**
CD83	CD83 molecule	17005001	**2.6**	0.020	0.217	**7.8**	0.001	**0.021**
SPANXC	SPANX family, member C	17114713	**2.3**	0.005	0.109	**7.7**	<0.001	**0.010**
GADD45B	Growth arrest and DNA-damage-inducible, beta	16856803	**2.8**	0.003	0.088	**7.7**	<0.001	**0.010**
RNU12	RNA, U12 small nuclear	16930938	**4.6**	0.002	0.063	**7.1**	<0.001	**0.015**
DUSP1	Dual specificity phosphatase 1	17002846	**4.7**	0.002	0.067	**6.9**	0.001	**0.019**
SESN2	Sestrin 2	16661544	**2.9**	0.017	0.198	**6.8**	0.002	**0.031**
PPP1R15A	Protein phosphatase 1, regulatory subunit 15A	16863877	**2.9**	0.049	0.335	**6.7**	0.002	**0.036**
AVPI1	Arginine vasopressin-induced 1	16717235	**4.2**	0.001	0.044	**6.6**	<0.001	**0.008**
RNU5B-1	RNA, U5B small nuclear 1	16802102	**2.7**	<0.001	0.018	**6.6**	<0.001	**0.014**
ABTB2	Ankyrin repeat and BTB (POZ) dc2	16737260	**3.6**	<0.001	0.033	**6.5**	<0.001	**0.006**
PTGS2	Prostaglandin-endoperoxide synthase 2	16697370	**4.0**	0.004	0.093	**6.4**	0.001	**0.023**
PER1	Period circadian clock 1	16840846	**3.1**	0.015	0.183	**6.4**	0.002	**0.028**
SNORA14B	Small nucleolar RNA, H/ACA box 14B	16700713	**2.9**	0.004	0.096	**6.3**	<0.001	**0.015**
LIPG	Lipase, endothelial	16852296	**2.5**	0.007	0.126	**6.2**	<0.001	**0.014**
SERTAD1	SERTA domain containing 1	16872443	**2.8**	0.001	0.058	**6.1**	<0.001	**0.006**
NR4A3	Nuclear receptor subfamily 4, group A, member 3	17087517	**2.9**	<0.001	0.042	**6.0**	<0.001	**0.007**
SNORD14E	Small nucleolar RNA, C/D box 14E	16745561	**2.2**	<0.001	0.016	**5.9**	<0.001	**0.003**
SLCO4C1	Solute carrier organic anion transporter 4C1	16998551	**4.1**	0.001	0.045	**5.8**	<0.001	**0.010**
MYLIP	Myosin regulatory light chain interacting protein	17005077	**3.2**	<0.001	0.026	**5.8**	<0.001	**0.006**
IL6R	Interleukin 6 receptor	16671457	**4.0**	<0.001	0.021	**5.8**	<0.001	**0.008**
MYC	v-Myc avian myelocytomatosis viral oncogene	17072669	**2.6**	0.013	0.171	**5.8**	0.001	**0.024**
NR4A1	Nuclear receptor subfamily 4, group A, member 1	16751438	**2.1**	0.001	0.044	**5.7**	<0.001	**0.004**
INSIG1	Insulin induced gene 1	17053892	**3.0**	<0.001	0.019	**5.5**	<0.001	**0.003**
STX11	Syntaxin 11	17013279	**2.3**	0.012	0.165	**5.5**	<0.001	**0.006**
HSPA1A; 1B	Heat shock 70kDa protein 1A;1B	17006863	**2.3**	0.001	0.059	**5.5**	<0.001	**0.004**
NR4A2	Nuclear receptor subfamily 4, gA, m 2	16903897	**3.0**	<0.001	0.018	**5.5**	<0.001	**0.004**
GEM	GTP binding protein	17079210	**2.6**	<0.001	0.023	**5.5**	<0.001	**0.005**
HSPA1A; 1B	Heat shock 70kDa protein 1B;1A	17006881	**2.1**	0.001	0.057	**5.4**	<0.001	**0.004**
CLCF1	Cardiotrophin-like cytokine factor 1	16740969	**3.5**	0.019	0.208	**5.4**	0.004	**0.046**
FBXO32	F-box protein 32	17080788	**3.6**	<0.001	0.017	**5.3**	<0.001	**0.004**
RGCC	Regulator of cell cycle	16774303	**2.7**	0.003	0.081	**5.2**	<0.001	**0.015**
FOXC1	Forkhead box C1	17004208	**3.3**	0.001	0.056	**5.1**	<0.001	**0.014**
BHLHE40	Basic helix-loop-helix family, member e40	16937024	**5.3**	<0.001	0.022	**5.0**	<0.001	**0.007**
KDM7A	Lysine (K)-specific demethylase 7A	17063507	**2.8**	<0.001	0.026	**5.0**	<0.001	**0.005**

Table I. *Continued*

Table I. *Continued*

Down-regulated by YM-155			8-hour			20-hour		
Gene Symbol	Description	Cluster ID	FC at 8 h	ANOVA *p*-value	FDR *p*-value	FC at 20 h	ANOVA *p*-value	FDR *p*-value
GUSBP3	Glucuronidase, beta pseudogene 3	16996969	-3.6	0.035	0.283	-12.2	0.007	**0.061**
MIRLET7A2	microRNA let-7a-2	16745507	-4.1	0.001	0.050	-10.1	<0.001	**0.012**
CENPI	Centromere protein I	17105401	-2.0	0.001	0.057	-9.3	<0.001	**0.004**
SERTAD4	SERTA domain containing 4	16677071	-3.1	0.001	0.055	-6.5	<0.001	**0.012**
POLQ	Polymerase (DNA directed), theta	16957951	-2.1	0.001	0.058	-6.5	<0.001	**0.014**
POLE2	Polymerase (DNA directed), epsilon 2	16792519	-2.1	<0.001	0.028	-5.9	<0.001	**0.008**
ZFYVE28	Zinc finger, FYVE domain containing 28	16973753	-2.8	0.008	0.138	-5.8	0.001	**0.021**
PRIM1	Primase, DNA, polypeptide 1 (49kDa)	16766318	-2.2	<0.001	0.019	-4.8	<0.001	**0.007**
BORA	Bora, aurora kinase A activator	16775324	-2.7	0.011	0.156	-4.7	0.001	**0.024**
LMNB1	Lamin B1	16988703	-2.3	<0.001	0.017	-4.6	<0.001	**0.003**
ARHGAP11B	Rho GTPase activating protein 11B	16798812	-2.6	0.001	0.048	-4.6	0.004	**0.046**
RAD54B; FSBP	RAD54 homolog B; fibrinogen sbp	17079220	-2.0	<0.001	0.020	-4.5	<0.001	**0.006**
HIST1H2AI	Histone cluster 1, H2ai	17005858	-2.2	<0.001	0.026	-4.4	0.001	**0.023**
MIR454	microRNA 454	16847249	-2.4	0.013	0.173	-4.3	0.001	**0.025**
SKP2	S-phase kinase-associated protein 2, E3 UPL	16984032	-2.3	<0.001	0.020	-4.3	<0.001	**0.005**
ZNF724P	Zinc finger protein 724, pseudogene	16870925	-3.2	0.004	0.101	-4.2	0.001	**0.017**
CDCA7	Cell division cycle associated 7	16887840	-2.4	0.003	0.082	-4.1	<0.001	**0.009**
CDC7	Cell division cycle 7	16667037	-2.0	0.001	0.047	-4.0	<0.001	**0.004**
GPR180	G protein-coupled receptor 180	16775823	-2.2	<0.001	0.035	-4.0	<0.001	**0.008**
RMI1	RecQ mediated genome instability 1	17086353	-2.0	0.002	0.070	-3.9	<0.001	**0.009**
MIR21; VMP1	microRNA 21; vacuole membrane protein 1	16836624	-4.2	<0.001	0.042	-3.8	0.001	**0.022**
MIR125B1	microRNA 125b-1	16745501	-2.3	0.017	0.194	-3.5	<0.001	**0.003**
MIR181B1	microRNA 181b-1	16697660	-2.1	0.007	0.127	-3.4	0.001	**0.016**

The data in this study show only a small reduction of survivin within 8 h of treatment, despite enormous global changes to the transcriptome, some of which are exacerbated by 20 hours coinciding with cell death. Table I shows only the changes evident in BOTH groups, where as individual datasets for control and treatment (8 h) and (20 h) have been deposited with NCBI's Gene Expression Omnibus which are accessible through GEO Series accession number GSE103089 located at https://www.ncbi.nlm.nih.gov/geo/query/acc.cgi?acc=GSE103089.

Up-regulation of tumor suppressors. YM-155 elicited enormous differential transcript changes some consistently observed at both 8 and 20-hour time points to which many of these correspond to under-researched transcripts of unknown function. Some of these include the YM-155 mediated up-regulation of tumor suppressor: FBJ murine osteosarcoma viral oncogene homolog B (FOSB) [+12.42, $p<0.001$, 8 h]. While little is known about FOSB, it is reportedly under-expressed in malignant tumors (39, 40) with lower levels predicting aggressive metastasis, cell proliferation, clonal formation and overall poor patient survival rates (41). In contrast, the up-regulation of FOSB would afford greater chemo-sensitivity to tumoricidal peptides or anthracyclines (42) and favorable recurrence-free survival in cases of breast cancer (43). More research will be required to investigate not only a role for FOSB in diverse cancers, but also how YM-155 can influence over this gene. Another example of a relatively under-studied transcript up-regulated by YM-155, is salt inducible kinase 1 (SIK1) which is evident at both time points [+5.04, $p<0.001$, 8 h/ +8.06, $p<0.001$, 20 h]. Like FOSB, SIK1 has been reported as a tumor suppressor capable of halting tumor growth, metastasis and rendering greater overall survival rates (44, 45). Likewise, numerous studies are now reporting that a reduction of SIK1 is associated with drug/adiation resistance, aggressive tumor pathologies and greater likelihood of epithelial–mesenchymal transition (46-48). Again, more work is needed to investigate not only a role for SIK1 in diverse cancers, but the YM-155 influence over this gene. Yet, another example of a YM-155 target gene to which little is known, is that of up-regulated expression of tumor necrosis factor, alpha-induced protein 3 (TNFAIP3) [+18.08, $p<0.001$]. What we do know from previous research is that low levels of TNFAIP3 are related to germline

mutations associated with a plethora of inflammatory diseases (49) such as arthritis, myasthenia gravis (50) autoimmune hepatitis (51) autoimmune lymphoproliferative syndrome (52) and T-cell acute lymphoblastic leukemia (53, 54). TNFAIP3 functions an endogenous anti-inflammatory regulator with capacity to down-regulate nuclear factor kappaB signaling, (52) attenuate suppressor of cytokine signaling 3 (55) and JNK phosphorylation (56), with its overexpression triggering tumor apoptosis, and reduction in cytokine release as well as metastasis/migration/ invasion (57-60).

Future research on many of these transcripts (Table I) is required to unveil the most influential aspect of this drug. The boundaries of this discussion will now focus on the known major pathways affected by YM-155 in MDA-MB-231 cells at the 20 hr time point. The data shows significant impact primarily on reduction in genomic stability, with broad scale changes in pathway elements associated with DNA replication, DNA damage response pathways (DDR) and cell cycle (Figure 9-11) rather than a loss of survivin and its role in apoptosis (Figure 11).

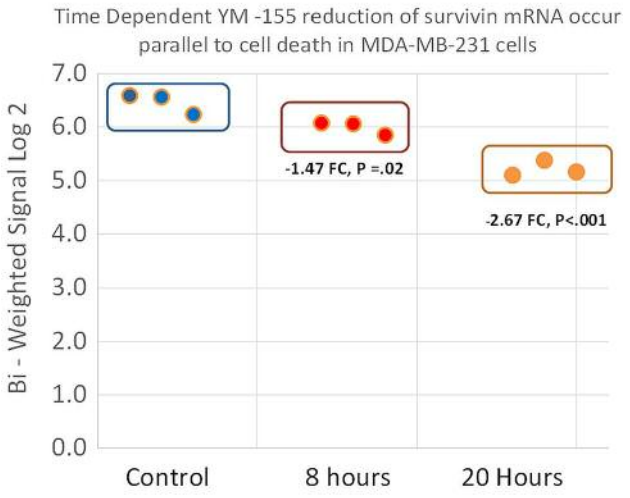

Figure 7. *Survivin mRNA transcript change in YM-155 treated cells 8 h (83 ng/mL) and 20 h (14.6 ng/mL). The data represent raw data triplicate microarray spot values by intensity presented as bi-weighted average Signal (log2) for the BIRC5/baculoviral IAP repeat containing 5 gene.*

DNA damage pathway. YM-155 caused numerous down-regulated processes at 20 h which are otherwise required to overcome damaged DNA at the stalled replication fork through two central kinase controlled signaling pathways 1) ATR (ATM- and Rad3-Related) and 2) ATM (ataxia-telangiectasia mutated) (Figure 9). Loss of function in both ATR and ATM would render faulty repair of replication-associated DNA damage and DNA double-strand breaks, to which YM-155 mediated a significant reduction key player, such as Fanconi complementation group D2 (FANCD2) [–7.16, $p<0.001$]. This particular gene is linked to the control of hypersensitivity to the damaging effects of crosslinking agents of DNA. A genetic inherited recessive mutation of FANCD2 in the germline creates major chromosomal instability where FANCD2$^{-/-}$ or a single mutation in BRCA2 [–5.98, $p<0.001$] are associated with replicative DNA errors and greater risk of diverse cancers including ovarian, head and neck and breast (61). Once cancers are established, anti-cancer drugs that impair the damaged DNA response pathways such as DNA interstrand crosslinking (ICL) agents are employed like cisplatin, mitomycin C or related chemotherapy drugs (62). The results of this study suggest this could on of the primary mechanisms for YM-155 mediated lethal effects on breast cancer cells.

Moreover, according to Figure 9 and the GEO 20 h full dataset: the data show a YM-155 mediated reduction in not only FANCD2 expression – but also many of the Fanconi anemia E3 monoubiquitin ligase core complex components (FANCA/B/C/E/F/G/L/M): group A (FANCA [–4.03, $p<0.001$], group B (FANCB [–3.34, $p<0.001$]), group L ANCL [–4.21, $p<0.001$]), group E (FANCE [–2.02, $p<0.001$]), group F (FANCF [–2.17, $p<0.001$], group G (FANCG [–2.28, $p<0.001$]) group M (FANCM [–3.62, $p<0.001$]) all of which are needed to activate FANCD2 through ubiquitination. A loss of ubiquitinated FANCD2 renders inadequate formation of the FANCD2/FANCI complex [–8.56, $p<0.001$] which is needed to initiate DNA repair by driving formation of the multicomplex BRCA1 [–3.14, $p<0.001$], BRAC2 and RAD51 [–3.74, $p<0.001$], which were themselves also affected. Just a single target impact on one of these systems alone (*e.g.* FANCD2 monoubiquitination) can augment existing chemotherapies of the ICL class (61, 63). YM-155 appears to be a multi-target drug with major effects on DNA repair.

Even further, in regards to DNA damage response, YM-155 also caused reduction in downstream elements of the ATM/FANCD2 pathway. An example of this is the reduced transcript for PRKDC [–3.3, $p<0.001$], which would fail to activate CHEK2 to phosphorylate and activate BRAC1. Failure in this particular step would prevent complex formation of ubiquitinated FANCD2 to BRCA1 and RAD51 and halt the DDR. Not only this, but YM-155 also adversely affects the partner and localizer of BRCA2 (PALB2 [–2.33, $p<0.001$]), which is required for protein linking BRCA1, BRCA2 and RAD51 at the site of a DNA double-strand break. This is pivotal because a combined reduction of BRCA1 interacting protein C-terminal helicase 1, BRIP1 [–6.37, p=6.43E-07] (FANCJ) at both time points would prevent its role as a major helicase needed to interact with BRCA1 to oversee homologous recombination DNA repair and cell response to replication stresses (64). Although many more targets are centered around YM-155 mediated impairment to the DNA damage response pathway, as a last

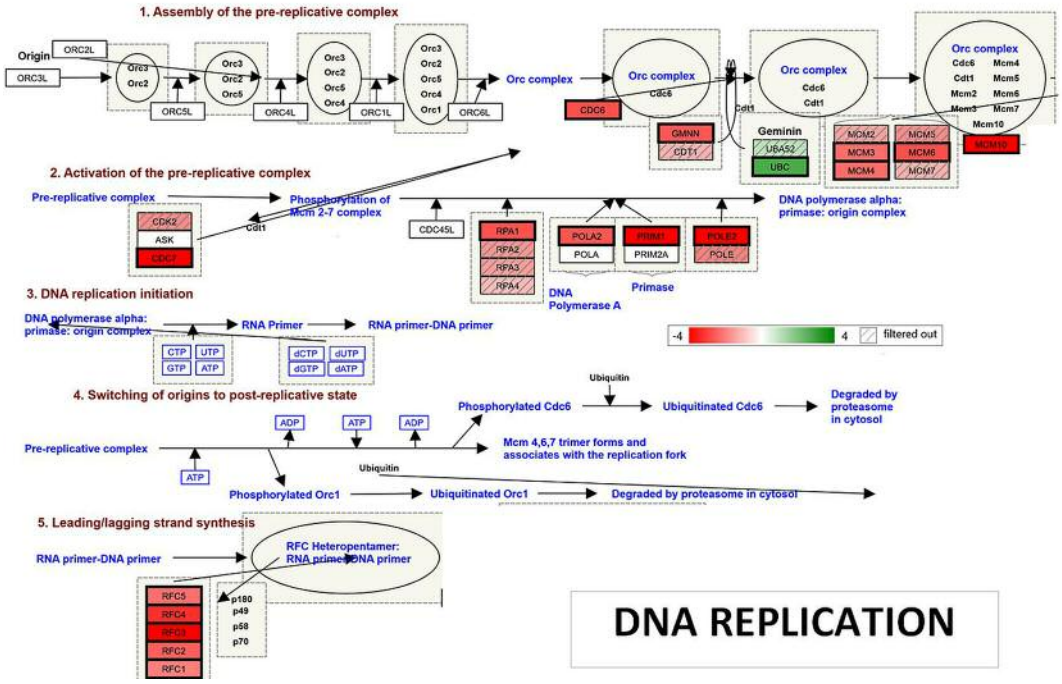

Figure 8. *DNA REPLICATION: YM-155 affected pathway elements at 20 h (14.6 ng/mL) in MDA-MB-231 cells. Down-regulated transcripts are denoted by solid red, up-regulated transcripts by solid green, and ///// no statistical differences.*

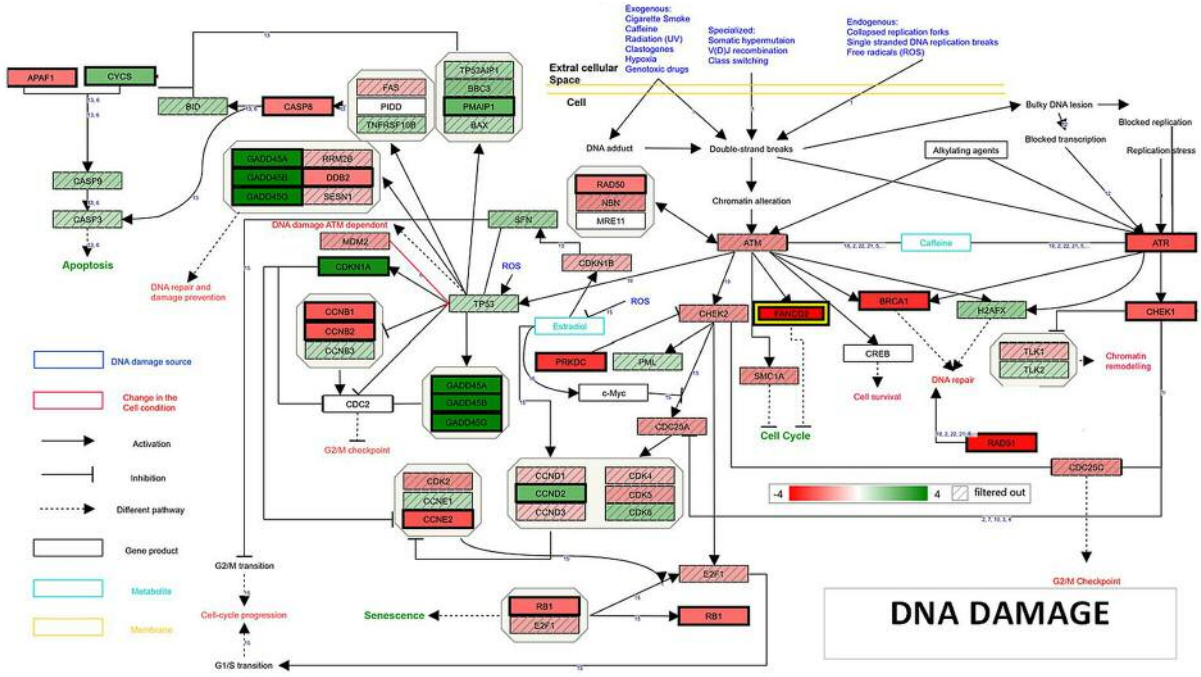

Figure 9. *DNA DAMAGE: YM-155 affected pathway elements at 20 h (14.6 ng/mL) in MDA-MB-231 cells. Down-regulated transcripts are denoted by solid red, up-regulated transcripts by solid green, and ///// no statistical differences.*

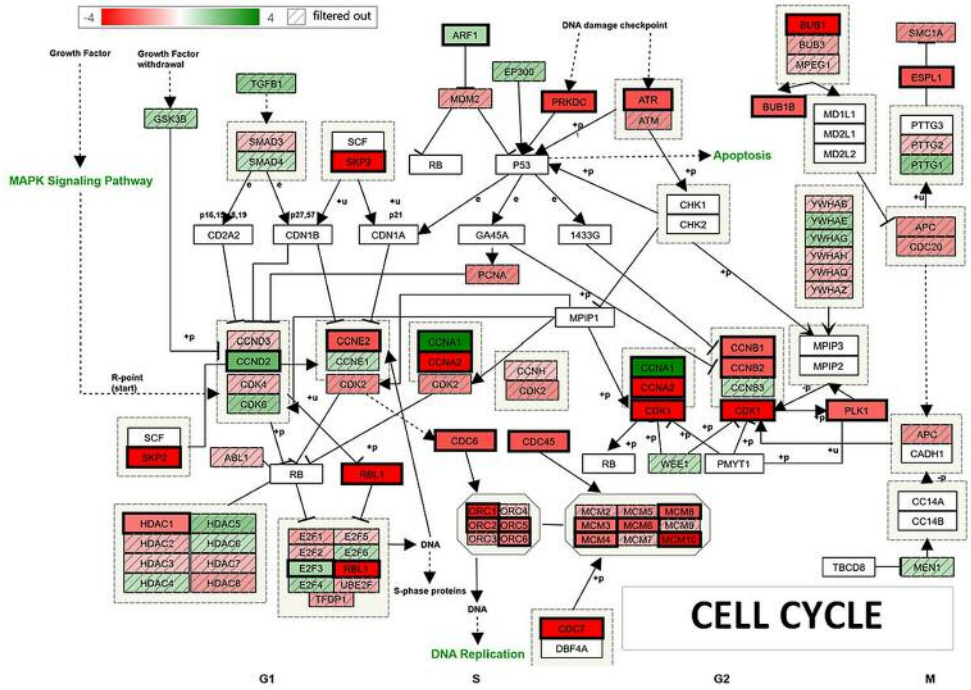

Figure 10. *CELL CYCLE: YM-155 affected pathway elements at 20 h (14.6 ng/mL) in MDA-MB-231 cells. Down-regulated transcripts are denoted by solid red, up-regulated transcripts by solid green, and ///// no statistical differences.*

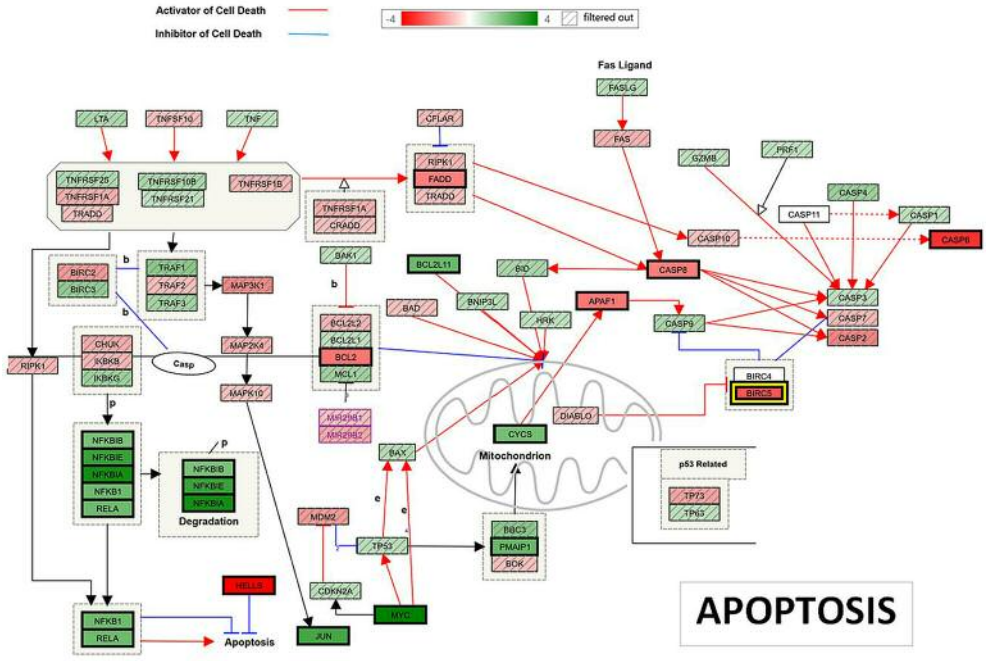

Figure 11. *APOPTOSIS: YM-155 affected pathway elements at 20 h (14.6 ng/mL). Down-regulated transcripts are denoted by solid red, up-regulated transcripts by solid green, and ///// no statistical differences.*

example, we see reduction in exonuclease 1 (EXO1 [–4.57, $p<0.001$]) which is required for 5' resection in DNA mismatch repair processes involving homologous recombination repair at stalled replication forks (65-67). Lastly, YM-155 simultaneously down-regulated up/stream and downstream targets of EXO1 such as ATM, ATR and cyclin-dependent kinases 1[–4.09, $p<0.001$] and 2 findings which all corroborate major impact on DNA damage response. A significant loss of these processes would augment effects of chemotherapy, radiotherapy, and poly(ADP-ribose) polymerase inhibitors (68). These findings suggest a very potent role of YM-155 to destabilize integrity of the genome through direct genetic repression of Fanconi anemia pathways transcript components – all of which would lead to inability to repair DNA (69).

DNA replication. YM-155 also influenced down-regulation of transcripts associated with the assembly of the pre-replicative complex/CDC6 [–2.82, $p<0.001$], GMNN [–2.18, $p<0.001$] and several mini-chromosome maintenance helicases (MCM) transcripts. Cell cycle protein CDC6 is involved with recruiting MCMs 2-7 onto the origin recognition complex (ORC), then licensed for replication (70, 71). YM-155 caused losses in processes associated with the activation of the ORC in particular by down-regulating CDC7 [–3.95, $p<0.001$] needed to phosphorylate MCM proteins during the S phase for activation of the replication initiation complex assembly (72, 73). Losses of POLA2 [–2.74, $p<0.001$] would render the reduction in DNA synthesis, which could be beneficial to augment effects of chemotherapies such as gemcitabine in resistant cell lines (74). YM-155 also caused simultaneous reduction in the polymerase complex (POLA/primase) PRIM1 [–2.17, $p<0.001$] and POLE2 [–2.68, $p=0.004308$] which could lead to faulty telomere processing (75). In addition, YM-155 triggered negative changes in the RNA primer-DNA primer with losses in replication factor C (RFC) including both the large subunit [replication factor C, subunit 1 (RFC1)] [–2.14, $p<0.001$] and four small subunits [replication factor C, subunits 2-5 (RFC25)], which could lead to impaired activation of DNA polymerases [6] through inadequate loading of PCNA onto chromatin and DNA polymerases to PCNA (76-78), Several of these changes overlap onto the YM-155 effects on cell cycle (Figure 10).

Cell cycle. In response to DNA damage, cells are arrested through replication stress by down-regulating the activity of cyclin-dependent kinases (CDKs) and cell cycle kinases, including Polo-like kinase 1 (PLK1) [–2.41, $p<0.001$], Bora [–4.56, $p<0.001$] and Aurora kinases (79). In this study, YM-155 mediated a loss of many of these processes including CCNB1 [–2.5, $p<0.001$] and CCNB2 [–2.77, $p<0.001$] (which encodes G2/mitotic-specific cyclin-B 1 and 2 proteins) cyclin B/CDK1, BORA, AURKB, CENPA, CCNE2 and its target PLK1 [–2.41, $p<0.001$], all of which are essential for mitotic recovery after DNA damage (80-85). Many of these cycle checkpoint transcripts are reportedly overexpressed in aggressive chemo resistant tumors (86-91) leading to unbridled proliferation (92), poor prognosis (93) to which small-molecule inhibitors that target these kinases are currently being tested as anticancer drugs (94-96). Kinase inhibition would indirectly prevent Plk1 activation, initiate G2 arrest (97), trigger a simultaneous rise in tumor suppressors- p53-inducible p21 tumor, Wee1, Myt1, p21 (98), as well as proteasomal Bcl-2 degradation (99) all contributing to cytostatic mediated apoptosis (100-107). YM-155 appears to down-regulate this mitotic cascade through attenuating transcript levels of related kinases.

The data from this work also shows that YM-155 mediates a loss in (budding uninhibited by benzimidazoles 1) BUB1 [–5.95, $p<0.001$]/BUB1B which could block not only checkpoint activity leading to mitosis but also spindle assembly, kinetochore–microtubule attachment and chromosome segregation (88, 108, 109). Other related transcripts down-regulated by YM-155 include SKP2 [–2.23, $p<0.001$] which encodes for S-phase kinase-associated protein 2 which is part of SCF complex (SKp1-cullin-FBox)/Cks1 inversely associated with concentration of p27Kip1 and p57Kip2 (CDK inhibitors) which initiate cell cycle arrest (110, 111).

Clinical Application

While the data in this study support existing literature describing the lethal effects of YM-155 on tumor cells *in vitro*, its clinical application remains uncertain. The National Institutes of Health website, ClinicalTrials.gov, lists 11 clinical trials using YM-155. Most of these are phase I and II trials assessing tolerability and dosing with few powered to study clinical efficacy against cancer. Phase II trials evaluating adjunctive use with standard treatments such as rituximab (relapsed aggressive B-cell non-Hodgkin lymphoma), carboplatin and paclitaxel (lung cancer) or docetaxel (HER2 negative breast cancer) show adequate tolerability with moderate to no clinical improvements with side effects including alopecia, fatigue, nausea, decreased hemoglobin/anemia, headache and neutropenia (112-117). It appears unlikely that YM-155 will be useful as an add-on medication in advanced late-stage metastatic disease. Perhaps a clearer understanding the actions of this drug, higher levels of tolerated dose and understanding its biological stability will allow a rational deployment in which it has efficacy.

In conclusion, the data from this work provide a framework circumscribing the entire transcriptome differential response to YM-155 in TNBC cells. This data can serve as a reference point for future work on defining a more finite and concrete

mechanism for this drug. Clearly, YM-155 exerts dynamic global effects on the transcriptome, affecting hundreds if not thousands of processes independent of survivin and inclusive to major negative impact on DNA replication, cell cycle and DNA damage would exert negative controlling influence over tumor growth and augment effects of ICL chemotherapy agents (63, 118). The findings in this study can be further explored using the public dataset, and functional biological algorithms in NCBI's Gene Expression Omnibus and are accessible through GEO Series accession number GSE103089 located https://www.ncbi.nlm.nih.gov/geo/query/acc.cgi?acc=GSE103089.

Conflicts of Interest

The Authors wish to confirm that there are no known conflicts of interest associated with this publication and there has been no significant financial support for this work that could have influenced its outcome.

Acknowledgements

This project was supported by the National Institutes of Health, National Institute on Minority Health and Health Disparities, RCMI grant (8G12MD007582-28.) and COE grant (P20 MD006738). We also wish to thank Dr. Shawn Lee Thomas and students: Davonta Powe and Anthony A Jumelles from the Dept. of Biology / Florida A&M University for their support and assistance.

References

1 Ambrosini G, Adida C and Altieri DC: A novel anti-apoptosis gene, survivin, expressed in cancer and lymphoma. Nat Med *3(8)*: 917-921, 1997.

2 Reis FR, Vasconcelos FC, Pereira DL, Moellman-Coelho A, Silva KL and Maia RC: Survivin and p-glycoprotein are associated and highly expressed in late phase chronic myeloid leukemia. Oncol Rep *26(2)*: 471-478, 2011.

3 Liang QL, Wang BR and Li GH: Dcr3 and survivin are highly expressed in colorectal carcinoma and closely correlated to its clinicopathologic parameters. J Zhejiang Univ Sci B *10(9)*: 675-682, 2009.

4 Schmidt SM, Schag K, Muller MR, Weck MM, Appel S, Kanz L, Grunebach F and Brossart P: Survivin is a shared tumor-associated antigen expressed in a broad variety of malignancies and recognized by specific cytotoxic t cells. Blood *102(2)*: 571-576, 2003.

5 Marioni G, Brescia G, Nicole L, Marchese-Ragona R, Barion U, Giacomelli L, Marino F, Martini A and Ottaviano G: Survivin and cortactin expression in sinonasal schneiderian (inverted) papilloma and associated carcinoma. Am J Rhinol Allergy *32(2)*: 78-81, 2018.

6 Nasu S, Yagihashi A, Izawa A, Saito K, Asanuma K, Nakamura M, Kobayashi D, Okazaki M and Watanabe N: Survivin mrna expression in patients with breast cancer. Anticancer Res *22(3)*: 1839-1843, 2002.

7 Peery RC, Liu JY and Zhang JT: Targeting survivin for therapeutic discovery: Past, present, and future promises. Drug Discov Today *22(10)*: 1466-1477, 2017.

8 Unruhe B, Schroder E, Wunsch D and Knauer SK: An old flame never dies: Survivin in cancer and cellular senescence. Gerontology *62(2)*: 173-181, 2016.

9 Xia R, Chen S, Chen Y, Zhang W, Zhu R and Deng A: A chromosomal passenger complex protein signature model predicts poor prognosis for non-small-cell lung cancer. Onco Targets Ther *8*: 721-726, 2015.

10 Kennedy SM, O'Driscoll L, Purcell R, Fitz-Simons N, McDermott EW, Hill AD, O'Higgins NJ, Parkinson M, Linehan R and Clynes M: Prognostic importance of survivin in breast cancer. Br J Cancer *88(7)*: 1077-1083, 2003.

11 Xu C, Yamamoto-Ibusuki M, Yamamoto Y, Yamamoto S, Fujiwara S, Murakami K, Okumura Y, Yamaguchi L, Fujiki Y and Iwase H: High survivin mrna expression is a predictor of poor prognosis in breast cancer: A comparative study at the mrna and protein level. Breast Cancer *21(4)*: 482-490, 2014.

12 Zhang M, Zhang X, Zhao S, Wang Y, Di W, Zhao G, Yang M and Zhang Q: Prognostic value of survivin and egfr protein expression in triple-negative breast cancer (tnbc) patients. Target Oncol *9(4)*: 349-357, 2014.

13 Nakahara T, Kita A, Yamanaka K, Mori M, Amino N, Takeuchi M, Tominaga F, Kinoyama I, Matsuhisa A, Kudou M and Sasamata M: Broad spectrum and potent antitumor activities of ym155, a novel small-molecule survivin suppressant, in a wide variety of human cancer cell lines and xenograft models. Cancer Sci *102(3)*: 614-621, 2011.

14 Yamanaka K, Nakata M, Kaneko N, Fushiki H, Kita A, Nakahara T, Koutoku H and Sasamata M: Ym155, a selective survivin suppressant, inhibits tumor spread and prolongs survival in a spontaneous metastatic model of human triple negative breast cancer. Int J Oncol *39(3)*: 569-575, 2011.

15 Cheng SM, Chang YC, Liu CY, Lee JY, Chan HH, Kuo CW, Lin KY, Tsai SL, Chen SH, Li CF, Leung E, Kanwar JR, Huang CC, Chang JY and Cheung CH: Ym155 down-regulates survivin and xiap, modulates autophagy and induces autophagy-dependent DNA damage in breast cancer cells. Br J Pharmacol *172(1)*: 214-234, 2015.

16 Nitta T, Koike H, Miyao T, Miyazawa Y, Kato H, Furuya Y, Sekine Y and Suzuki K: Ym155 reverses statin resistance in renal cancer by reducing expression of survivin. Anticancer Res *37(1)*: 75-80, 2017.

17 Manouchehri JM and Kalafatis M: Sensitization of rhtrail-resistant triple-negative breast carcinoma through silibinin co-treatment. Anticancer Res *37(12)*: 6593-6599, 2017.

18 Takeda H, Okada M, Suzuki S, Kuramoto K, Sakaki H, Watarai H, Sanomachi T, Seino S, Yoshioka T and Kitanaka C: Rho-associated protein kinase (rock) inhibitors inhibit survivin expression and sensitize pancreatic cancer stem cells to gemcitabine. Anticancer Res *36(12)*: 6311-6318, 2016.

19 Fragni M, Bonini SA, Stabile A, Bodei S, Cristinelli L, Simeone C, Zani D, Spano PF, Berruti A, Memo M and Sigala S: Inhibition of survivin is associated with zoledronic acid-induced apoptosis of prostate cancer cells. Anticancer Res *36(3)*: 913-920, 2016.

20 Yoon DH, Shin JS, Jin DH, Hong SW, Jung KA, Kim SM, Hong YS, Kim KP, Lee JL, Suh C, Lee JS and Kim TW: The survivin suppressant ym155 potentiates chemosensitivity to gemcitabine in the human pancreatic cancer cell line miapaca-2. Anticancer Res *32(5)*: 1681-1688, 2012.

21 Ashburner M, Ball CA, Blake JA, Botstein D, Butler H, Cherry JM, Davis AP, Dolinski K, Dwight SS, Eppig JT, Harris MA, Hill DP, Issel-Tarver L, Kasarskis A, Lewis S, Matese JC, Richardson JE, Ringwald M, Rubin GM and Sherlock G: Gene ontology: Tool for the unification of biology. The gene ontology consortium. Nat Genet *25(1)*: 25-29, 2000.

22 Voges Y, Michaelis M, Rothweiler F, Schaller T, Schneider C, Politt K, Mernberger M, Nist A, Stiewe T, Wass MN, Rodel F and Cinatl J: Effects of ym155 on survivin levels and viability in neuroblastoma cells with acquired drug resistance. Cell Death Dis *7(10)*: e2410, 2016.

23 Li KL, Wang YF, Qin JR, Wang F, Yang YT, Zheng LW, Li MH, Kong J, Zhang W and Yang HY: Rapamycin enhances the anti-angiogenesis and anti-proliferation ability of ym155 in oral squamous cell carcinoma. Tumour Biol *39(6)*: 1010428317706213, 2017.

24 Zhang S, Liu B, Fan Z, Wang D, Liu Y, Li J, Wang N, Liu Y and Zhang B: Targeted inhibition of survivin with ym155 promotes apoptosis of hypoxic human pulmonary arterial smooth muscle cells *via* the up-regulation of voltage-dependent k(+) channels. Mol Med Rep *13(4)*: 3415-3422, 2016.

25 Woo SM, Min KJ, Seo BR, Seo YH, Jeong YJ and Kwon TK: Ym155 enhances abt-737-mediated apoptosis through mcl-1 down-regulation in mcl-1-overexpressed cancer cells. Mol Cell Biochem *429(1-2)*: 91-102, 2017.

26 Ueno T, Uehara S, Nakahata K and Okuyama H: Survivin selective inhibitor ym155 promotes cisplatininduced apoptosis in embryonal rhabdomyosarcoma. Int J Oncol *48(5)*: 1847-1854, 2016.

27 Yu Y, Zhao X, Zhang Y, Kang Y, Wang J and Liu Y: Antitumor activity of ym155, a selective survivin suppressant, in combination with cisplatin in hepatoblastoma. Oncol Rep *34(1)*: 407-414, 2015.

28 Nakahara T, Yamanaka K, Hatakeyama S, Kita A, Takeuchi M, Kinoyama I, Matsuhisa A, Nakano K, Shishido T, Koutoku H and Sasamata M: Ym155, a novel survivin suppressant, enhances taxane-induced apoptosis and tumor regression in a human calu 6 lung cancer xenograft model. Anticancer Drugs *22(5)*: 454-462, 2011.

29 Gyuraszova K, Mikes J, Halaburkova A, Jendzelovsky R and Fedorocko P: Ym155, a small molecule inhibitor of survivin expression, sensitizes cancer cells to hypericin-mediated photodynamic therapy. Photochem Photobiol Sci *15(6)*: 812-821, 2016.

30 Cheng XJ, Lin JC, Ding YF, Zhu L, Ye J and Tu SP: Survivin inhibitor ym155 suppresses gastric cancer xenograft growth in mice without affecting normal tissues. Oncotarget *7(6)*: 7096-7109, 2016.

31 Zhang Z, Ma L and Wang J: Ym155 exerts a growth inhibitory effect on human osteosarcoma *in vitro* and *in vivo*. Oncol Rep *34(2)*: 1074-1080, 2015.

32 Zhang S, Wang X, Gu Z and Wang L: Small molecule survivin inhibitor ym155 displays potent activity against human osteosarcoma cells. Cancer Invest *34(8)*: 401-407, 2016.

33 Chuwa AH, Sone K, Oda K, Ikeda Y, Fukuda T, Wada-Hiraike O, Inaba K, Makii C, Takeuchi M, Oki S, Miyasaka A, Kashiyama T, Arimoto T, Kuramoto H, Kawana K, Yano T, Osuga Y and Fujii T: Significance of survivin as a prognostic factor and a therapeutic target in endometrial cancer. Gynecol Oncol *141(3)*: 564-569, 2016.

34 Zhao N, Mao Y, Han G, Ju Q, Zhou L, Liu F, Xu Y and Zhao X: Ym155, a survivin suppressant, triggers parp-dependent cell death (parthanatos) and inhibits esophageal squamous-cell carcinoma xenografts in mice. Oncotarget *6(21)*: 18445-18459, 2015.

35 Zhao X, Puszyk WM, Lu Z, Ostrov DA, George TJ, Robertson KD and Liu C: Small molecule inhibitor ym155-mediated activation of death receptor 5 is crucial for chemotherapy-induced apoptosis in pancreatic carcinoma. Mol Cancer Ther *14(1)*: 80-89, 2015.

36 Zhang L, Zhang W, Wang YF, Liu B, Zhang WF, Zhao YF, Kulkarni AB and Sun ZJ: Dual induction of apoptotic and autophagic cell death by targeting survivin in head neck squamous cell carcinoma. Cell Death Dis *6*: e1771, 2015.

37 Xia H, Chen J, Shi M, Deivasigamani A, Ooi LL and Hui KM: The over-expression of survivin enhances the chemotherapeutic efficacy of ym155 in human hepatocellular carcinoma. Oncotarget *6(8)*: 5990-6000, 2015.

38 Vequaud E, Seveno C, Loussouarn D, Engelhart L, Campone M, Juin P and Barille-Nion S: Ym155 potently triggers cell death in breast cancer cells through an autophagy-nf-kb network. Oncotarget *6(15)*: 13476-13486, 2015.

39 Milde-Langosch K, Kappes H, Riethdorf S, Loning T and Bamberger AM: Fosb is highly expressed in normal mammary epithelia, but down-regulated in poorly differentiated breast carcinomas. Breast Cancer Res Treat *77(3)*: 265-275, 2003.

40 Kataoka F, Tsuda H, Arao T, Nishimura S, Tanaka H, Nomura H, Chiyoda T, Hirasawa A, Akahane T, Nishio H, Nishio K and Aoki D: Egri and fosb gene expressions in cancer stroma are independent prognostic indicators for epithelial ovarian cancer receiving standard therapy. Genes Chromosomes Cancer *51(3)*: 300-312, 2012.

41 Kim JH, Lee JY, Lee KT, Lee JK, Lee KH, Jang KT, Heo JS, Choi SH and Rhee JC: Rgs16 and fosb underexpressed in pancreatic cancer with lymph node metastasis promote tumor progression. Tumour Biol *31(5)*: 541-548, 2010.

42 Ting CH, Chen YC, Wu CJ and Chen JY: Targeting fosb with a cationic antimicrobial peptide, tp4, for treatment of triple-negative breast cancer. Oncotarget *7(26)*: 40329-40347, 2016.

43 Pfannschmidt J, Bade S, Hoheisel J, Muley T, Dienemann H and Herpel E: Identification of immunohistochemical prognostic markers for survival after resection of pulmonary metastases from colorectal carcinoma. Thorac Cardiovasc Surg *57(7)*: 403-408, 2009.

44 Qu C and Qu Y: Down-regulation of salt-inducible kinase 1 (sik1) is mediated by rnf2 in hepatocarcinogenesis. Oncotarget *8(2)*: 3144-3155, 2017.

45 Du WQ, Zheng JN and Pei DS: The diverse oncogenic and tumor suppressor roles of salt-inducible kinase (sik) in cancer. Expert Opin Ther Targets *20(4)*: 477-485, 2016.

46 Yao YH, Cui Y, Qiu XN, Zhang LZ, Zhang W, Li H and Yu JM: Attenuated lkb1-sik1 signaling promotes epithelial-mesenchymal transition and radioresistance of non-small cell lung cancer cells. Chin J Cancer *35*: 50, 2016.

47 Yao J, Li Z, Wang X, Xu P, Zhao L and Qian J: Mir-125a regulates chemo-sensitivity to gemcitabine in human pancreatic cancer cells through targeting a20. Acta Biochim Biophys Sin (Shanghai) *48(2)*: 202-208, 2016.

48 Ren ZG, Dong SX, Han P and Qi J: Mir-203 promotes proliferation, migration and invasion by degrading sik1 in pancreatic cancer. Oncol Rep *35(3)*: 1365-1374, 2016.

49 Yamaguchi R, Sakamoto A, Yamamoto T, Narahara S, Sugiuchi H, Hisada A, Katoh T and Yamaguchi Y: Di-(2-ethylhexyl) phthalate suppresses il-12p40 production by gm-csf-dependent macrophages *via* the pparalpha/tnfaip3/traf6 axis after lipopolysaccharide stimulation. Hum Exp Toxicol: 9603271177 14038, 2017.

50 Yang HW, Xie Y, Zhao Y, Sun L, Zhu X, Wang S, Zhang YQ, Lei P and Meng Y: Tnfaip3 gene rs7749323 polymorphism is associated with late onset myasthenia gravis. Medicine (Baltimore) *96(20)*: e6798, 2017.

51 Xu E, Cao H, Lin L and Liu H: Rs10499194 polymorphism in the tumor necrosis factor-alpha inducible protein 3 (tnfaip3) gene is associated with type-1 autoimmune hepatitis risk in chinese han population. PLoS One *12(4)*: e0176471, 2017.

52 Takagi M, Ogata S, Ueno H, Yoshida K, Yeh T, Hoshino A, Piao J, Yamashita M, Nanya M, Okano T, Kajiwara M, Kanegane H, Muramatsu H, Okuno Y, Shiraishi Y, Chiba K, Tanaka H, Bando Y, Kato M, Hayashi Y, Miyano S, Imai K, Ogawa S, Kojima S and Morio T: Haploinsufficiency of tnfaip3 (a20) by germline mutation is involved in autoimmune lymphoproliferative syndrome. J Allergy Clin Immunol *139(6)*: 1914-1922, 2017.

53 Zhou L, Zheng H, Huang X, Zhu L, Wu S, Zeng C, Yang L, Chen S, Luo G, Du X and Li Y: Different genetic alteration of a20 in a sezary syndrome case with valpha2-jalpha22 t cell clone. Asia Pac J Clin Oncol *(2)*: e116-e123, 2017.

54 Zhang L, Yuan X, Zhou Q, Shi J, Song Z, Quan R and Zhang D: Associations between tnfaip3 gene polymorphisms and rheumatoid arthritis risk: A meta-analysis. Arch Med Res *(4)*: 386-392, 2017.

55 Sun Y, Lin Z, Liu CH, Gong Y, Liegl R, Fredrick TW, Meng SS, Burnim SB, Wang Z, Akula JD, Pu WT, Chen J and Smith LEH: Inflammatory signals from photoreceptor modulate pathological retinal angiogenesis *via* c-fos. J Exp Med *214(6)*: 1753-1767, 2017.

56 Pinna F, Bissinger M, Beuke K, Huber N, Longerich T, Kummer U, Schirmacher P, Sahle S and Breuhahn K: A20/tnfaip3 discriminates tumor necrosis factor (tnf)-induced nf-kappab from jnk pathway activation in hepatocytes. Front Physiol *8*: 610, 2017.

57 Huang T, Yin L, Wu J, Gu JJ, Ding K, Zhang N, Du MY, Qian LX, Lu ZW and He X: Tnfaip3 inhibits migration and invasion in nasopharyngeal carcinoma by suppressing epithelial mesenchymal transition. Neoplasma *64(3)*: 389-394, 2017.

58 Salim H, Arvanitis A, de Petris L, Kanter L, Haag P, Zovko A, Ozata DM, Lui WO, Lundholm L, Zhivotovsky B, Lewensohn R and Viktorsson K: Mirna-214 is related to invasiveness of human non-small cell lung cancer and directly regulates alpha protein kinase 2 expression. Genes Chromosomes Cancer *52(10)*: 895-911, 2013.

59 Majumdar I, Ahuja V and Paul J: Altered expression of tumor necrosis factor alpha -induced protein 3 correlates with disease severity in ulcerative colitis. Sci Rep *7(1)*: 9420, 2017.

60 Liu Y, Ye Z, Li X, Anderson JL, Khan M, DaSilva D, Baron M, Wilson D, Bocoun V, Ivacic LC, Schrodi SJ and Smith JA: Genetic and functional associations with decreased anti-inflammatory tumor necrosis factor alpha induced protein 3 in macrophages from subjects with axial spondyloarthritis. Front Immunol *8*: 860, 2017.

61 Ishiai M, Sato K, Tomida J, Kitao H, Kurumizaka H and Takata M: Activation of the fa pathway mediated by phosphorylation and ubiquitination. Mutat Res *803-805*: 89-95, 2017.

62 Jun DW, Hwang M, Kim HJ, Hwang SK, Kim S and Lee CH: Ouabain, a cardiac glycoside, inhibits the fanconi anemia/brca pathway activated by DNA interstrand cross-linking agents. PLoS One *8(10)*: e75905, 2013.

63 Wang GZ, Liu YQ, Cheng X and Zhou GB: Celastrol induces proteasomal degradation of fancd2 to sensitize lung cancer cells to DNA crosslinking agents. Cancer Sci *106(7)*: 902-908, 2015.

64 Wu W, Togashi Y, Johmura Y, Miyoshi Y, Nobuoka S, Nakanishi M and Ohta T: Hp1 regulates the localization of fancj at sites of DNA double-strand breaks. Cancer Sci *107(10)*: 1406-1415, 2016.

65 Liu T and Huang J: DNA end resection: Facts and mechanisms. Genomics Proteomics Bioinformatics *14(3)*: 126-130, 2016.

66 Myler LR, Gallardo IF, Soniat MM, Deshpande RA, Gonzalez XB, Kim Y, Paull TT and Finkelstein IJ: Single-molecule imaging reveals how mre11-rad50-nbs1 initiates DNA break repair. Mol Cell *67(5)*: 891-898 e894, 2017.

67 Kim HS, Nickoloff JA, Wu Y, Williamson EA, Sidhu GS, Reinert BL, Jaiswal AS, Srinivasan G, Patel B, Kong K, Burma S, Lee SH and Hromas RA: Endonuclease eepd1 is a gatekeeper for repair of stressed replication forks. J Biol Chem *292(7)*: 2795-2804, 2017.

68 Sundar R, Brown J, Ingles Russo A and Yap TA: Targeting atr in cancer medicine. Curr Probl Cancer *41(4)*: 302-315, 2017.

69 Nepomuceno TC, De Gregoriis G, de Oliveira FMB, Suarez-Kurtz G, Monteiro AN and Carvalho MA: The role of palb2 in the DNA damage response and cancer predisposition. Int J Mol Sci *18(9)*: pii: E1886, 2017.

70 Caillat C and Perrakis A: Cdt1 and geminin in DNA replication initiation. Subcell Biochem *62*: 71-87, 2012.

71 Nishitani H and Lygerou Z: Control of DNA replication licensing in a cell cycle. Genes Cells *7(6)*: 523-534, 2002.

72 Murai S, Katagiri Y and Yamashita S: Maturation-associated dbf4 expression is essential for mouse zygotic DNA replication. Dev Growth Differ *56(9)*: 625-639, 2014.

73 Seoane AI and Morgan DO: Firing of replication origins frees dbf4-cdc7 to target eco1 for destruction. Curr Biol *27(18)*: 2849-2855 e2842, 2017.

74 Koh V, Kwan HY, Tan WL, Mah TL and Yong WP: Knockdown of pola2 increases gemcitabine resistance in lung cancer cells. BMC Genomics *17(Suppl 13)*: 1029, 2016.

75 Diotti R, Kalan S, Matveyenko A and Loayza D: DNA-directed polymerase subunits play a vital role in human telomeric overhang processing. Mol Cancer Res *13(3)*: 402-410, 2015.

76 Overmeer RM, Gourdin AM, Giglia-Mari A, Kool H, Houtsmuller AB, Siegal G, Fousteri MI, Mullenders LH and Vermeulen W: Replication factor c recruits DNA polymerase delta to sites of nucleotide excision repair but is not required for pcna recruitment. Mol Cell Biol *30(20)*: 4828-4839, 2010.

77 Tang H, Hilton B, Musich PR, Fang DZ and Zou Y: Replication factor c1, the large subunit of replication factor c, is proteolytically truncated in hutchinson-gilford progeria syndrome. Aging Cell *11(2)*: 363-365, 2012.

78 Shiomi Y and Nishitani H: Control of genome integrity by rfc complexes; conductors of pcna loading onto and unloading from chromatin during DNA replication. Genes (Basel) *8(2)*: pii: E52, 2017.

79 Zou J, Rezvani K, Wang H, Lee KS and Zhang D: BRCA1 downregulates the kinase activity of polo-like kinase 1 in response to replication stress. Cell Cycle *12(14)*: 2255-2265, 2013.

80 Thomas Y, Cirillo L, Panbianco C, Martino L, Tavernier N, Schwager F, Van Hove L, Joly N, Santamaria A, Pintard L and Gotta M: CDK1 phosphorylates spat-1/bora to promote PLK1 activation in C. elegans and human cells. Cell Rep *15(3)*: 510-518, 2016.

81 Tavernier N, Panbianco C, Gotta M and Pintard L: CDK1 plays matchmaker for the polo-like kinase and its activator spat-1/bora. Cell Cycle *14(15)*: 2394-2398, 2015.

82 Tavernier N, Noatynska A, Panbianco C, Martino L, Van Hove L, Schwager F, Leger T, Gotta M and Pintard L: CDK1 phosphorylates spat-1/bora to trigger plk-1 activation and drive mitotic entry in C. Elegans embryos. J Cell Biol *208(6)*: 661-669, 2015.

83 Bruinsma W, Aprelia M, Kool J, Macurek L, Lindqvist A and Medema RH: Spatial separation of plk1 phosphorylation and activity. Front Oncol *5*: 132, 2015.

84 Bruinsma W, Macurek L, Freire R, Lindqvist A and Medema RH: Bora and aurora-a continue to activate plk1 in mitosis. J Cell Sci *127(Pt 4)*: 801-811, 2014.

85 Archambault V and Carmena M: Polo-like kinase-activating kinases: Aurora a, aurora b and what else? Cell Cycle *11(8)*: 1490-1495, 2012.

86 Bednarek K, Kiwerska K, Szaumkessel M, Bodnar M, Kostrzewska-Poczekaj M, Marszalek A, Janiszewska J, Bartochowska A, Jackowska J, Wierzbicka M, Grenman R, Szyfter K, Giefing M and Jarmuz-Szymczak M: Recurrent cdk1 overexpression in laryngeal squamous cell carcinoma. Tumour Biol *37(8)*: 11115-11126, 2016.

87 Ye Q, Lei L and Aili AX: Identification of potential targets for ovarian cancer treatment by systematic bioinformatics analysis. Eur J Gynaecol Oncol *36(3)*: 283-289, 2015.

88 Yan M, Song M, Bai R, Cheng S and Yan W: Identification of potential therapeutic targets for colorectal cancer by bioinformatics analysis. Oncol Lett *12(6)*: 5092-5098, 2016.

89 Zhang QQ, Chen J, Zhou DL, Duan YF, Qi CL, Li JC, He XD, Zhang M, Yang YX and Wang L: Dipalmitoylphosphatidic acid inhibits tumor growth in triple-negative breast cancer. Int J Biol Sci *13(4)*: 471-479, 2017.

90 Yang XR, Xiong Y, Duan H and Gong RR: Identification of genes associated with methotrexate resistance in methotrexate-resistant osteosarcoma cell lines. J Orthop Surg Res *10*: 136, 2015.

91 Sun Q, Shi R, Wang X, Li D, Wu H and Ren B: Overexpression of zic5 promotes proliferation in non-small cell lung cancer. Biochem Biophys Res Commun *479(3)*: 502-509, 2016.

92 Kaczorowski M, Borowiec T, Donizy P, Pagacz K, Fendler W, Lipinski A, Halon A and Matkowski R: Polo-like kinase-1 immunoreactivity is associated with metastases in cutaneous melanoma. J Cutan Pathol *44(10)*: 819-826, 2017.

93 Parrilla A, Cirillo L, Thomas Y, Gotta M, Pintard L and Santamaria A: Mitotic entry: The interplay between cdk1, plk1 and bora. Cell Cycle *15(23)*: 3177-3182, 2016.

94 Macurek L, Lindqvist A and Medema RH: Aurora-a and hbora join the game of polo. Cancer Res *69(11)*: 4555-4558, 2009.

95 Zhang QX, Gao R, Xiang J, Yuan ZY, Qian YM, Yan M, Wang ZF, Liu Q, Zhao HD and Liu CH: Cell cycle protein bora serves as a novel poor prognostic factor in multiple adenocarcinomas. Oncotarget *8(27)*: 43838-43852, 2017.

96 Bruinsma W, Aprelia M, Garcia-Santisteban I, Kool J, Xu YJ and Medema RH: Inhibition of polo-like kinase 1 during the DNA damage response is mediated through loss of aurora a recruitment by bora. Oncogene *36(13)*: 1840-1848, 2017.

97 Qin B, Gao B, Yu J, Yuan J and Lou Z: Ataxia telangiectasia-mutated- and rad3-related protein regulates the DNA damage-induced g2/m checkpoint through the aurora a cofactor bora protein. J Biol Chem *288(22)*: 16139-16144, 2013.

98 Jang SH, Kim AR, Park NH, Park JW and Han IS: Drg2 regulates g2/m progression *via* the cyclin b1-cdk1 complex. Mol Cells *39(9)*: 699-704, 2016.

99 Schwermer M, Dreesmann S, Eggert A, Althoff K, Steenpass L, Schramm A, Schulte JH and Temming P: Pharmaceutically inhibiting polo-like kinase 1 exerts a broad anti-tumour activity in retinoblastoma cell lines. Clin Exp Ophthalmol *45(3)*: 288-296, 2017.

100 Sydor S, Jafoui S, Wingerter L, Swoboda S, Mertens JC, Gerken G, Canbay A, Paul A and Fingas CD: Bcl-2 degradation is an additional pro-apoptotic effect of polo-like kinase inhibition in cholangiocarcinoma cells. World J Gastroenterol *23(22)*: 4007-4015, 2017.

101 Cheng YM, Tsai CC and Hsu YC: Sulforaphane, a dietary isothiocyanate, induces g(2)/m arrest in cervical cancer cells through cyclinb1 downregulation and gadd45beta/cdc2 association. Int J Mol Sci *17(9)*: pii: E1530, 2016.

102 Shi H, Li Y, Ren X, Zhang Y, Yang Z and Qi C: A novel quinazoline-based analog induces g2/m cell cycle arrest and apoptosis in human a549 lung cancer cells *via* a ros-dependent mechanism. Biochem Biophys Res Commun *486(2)*: 314-320, 2017.

103 Sano M, Ichimaru Y, Kurita M, Hayashi E, Homma T, Saito H, Masuda S, Nemoto N, Hemmi A, Suzuki T, Miyairi S and Hao H: Induction of cell death in pancreatic ductal adenocarcinoma by indirubin 3'-oxime and 5-methoxyindirubin 3'-oxime *in vitro* and *in vivo*. Cancer Lett *397*: 72-82, 2017.

104 Yi X, Li Y, Zai H, Long X and Li W: Klf8 knockdown triggered growth inhibition and induced cell phase arrest in human pancreatic cancer cells. Gene *585(1)*: 22-27, 2016.

105 Pan XW, Chen L, Hong Y, Xu DF, Liu X, Li L, Huang Y, Cui LM, Gan SS, Yang QW, Huang H, Qu FJ, Ye JQ, Wang LH and Cui XG: Eif3d silencing suppresses renal cell carcinoma tumorigenesis *via* inducing g2/m arrest through downregulation of cyclin b1/cdk1 signaling. Int J Oncol *48(6)*: 2580-2590, 2016.

106 Chang HT, Chou CT, Chen IS, Yu CC, Lu T, Hsu SS, Shieh P, Jan CR and Liang WZ: Mechanisms underlying effect of the mycotoxin cytochalasin b on induction of cytotoxicity, modulation of cell cycle, ca2+ homeostasis and ros production in human breast cells. Toxicology *370*: 1-19, 2016.

107 Schwermer M, Lee S, Koster J, van Maerken T, Stephan H, Eggert A, Morik K, Schulte JH and Schramm A: Sensitivity to cdk1-inhibition is modulated by p53 status in preclinical models of embryonal tumors. Oncotarget *6(17)*: 15425-15435, 2015.

108 Kulshrestha A, Suman S and Ranjan R: Network analysis reveals potential markers for pediatric adrenocortical carcinoma. Onco Targets Ther *9*: 4569-4581, 2016.

109 Kumar S, Sharma G, Chakraborty C, Sharma AR and Kim J: Regulatory functional territory of plk-1 and their substrates beyond mitosis. Oncotarget *8(23)*: 37942-37962, 2017.

110 Tomiatti V, Istvanffy R, Pietschmann E, Kratzat S, Hoellein A, Quintanilla-Fend L, von Bubnoff N, Peschel C, Oostendorp RA and Keller U: Cks1 is a critical regulator of hematopoietic stem cell quiescence and cycling, operating upstream of cdk inhibitors. Oncogene *34(33)*: 4347-4357, 2015.

111 Kamura T, Hara T, Kotoshiba S, Yada M, Ishida N, Imaki H, Hatakeyama S, Nakayama K and Nakayama KI: Degradation of p57kip2 mediated by scfskp2-dependent ubiquitylation. Proc Natl Acad Sci USA *100(18)*: 10231-10236, 2003.

112 Papadopoulos KP, Lopez-Jimenez J, Smith SE, Steinberg J, Keating A, Sasse C, Jie F and Thyss A: A multicenter phase II study of sepantronium bromide (ym155) plus rituximab in patients with relapsed aggressive b-cell non-hodgkin lymphoma. Leuk Lymphoma *57(8)*: 1848-1855, 2016.

113 Kelly RJ, Thomas A, Rajan A, Chun G, Lopez-Chavez A, Szabo E, Spencer S, Carter CA, Guha U, Khozin S, Poondru S, Van Sant C, Keating A, Steinberg SM, Figg W and Giaccone G: A phase i/ii study of sepantronium bromide (ym155, survivin suppressor) with paclitaxel and carboplatin in patients with advanced non-small-cell lung cancer. Ann Oncol *24(10)*: 2601-2606, 2013.

114 Clemens MR, Gladkov OA, Gartner E, Vladimirov V, Crown J, Steinberg J, Jie F and Keating A: Phase ii, multicenter, open-label, randomized study of ym155 plus docetaxel as first-line treatment in patients with her2-negative metastatic breast cancer. Breast Cancer Res Treat *149(1)*: 171-179, 2015.

115 Kudchadkar R, Ernst S, Chmielowski B, Redman BG, Steinberg J, Keating A, Jie F, Chen C, Gonzalez R and Weber J: A phase 2, multicenter, open-label study of sepantronium bromide (ym155) plus docetaxel in patients with stage iii (unresectable) or stage iv melanoma. Cancer Med *4(5)*: 643-650, 2015.

116 Lewis KD, Samlowski W, Ward J, Catlett J, Cranmer L, Kirkwood J, Lawson D, Whitman E and Gonzalez R: A multi-center phase ii evaluation of the small molecule survivin suppressor ym155 in patients with unresectable stage iii or iv melanoma. Invest New Drugs *29(1)*: 161-166, 2011.

117 Satoh T, Okamoto I, Miyazaki M, Morinaga R, Tsuya A, Hasegawa Y, Terashima M, Ueda S, Fukuoka M, Ariyoshi Y, Saito T, Masuda N, Watanabe H, Taguchi T, Kakihara T, Aoyama Y, Hashimoto Y and Nakagawa K: Phase i study of ym155, a novel survivin suppressant, in patients with advanced solid tumors. Clin Cancer Res *15(11)*: 3872-3880, 2009.

118 Karanja KK, Lee EH, Hendrickson EA and Campbell JL: Preventing over-resection by dna2 helicase/nuclease suppresses repair defects in fanconi anemia cells. Cell Cycle *13(10)*: 1540-1550, 2014.

Received April 11, 2018
Revised May 16, 2018
Accepted May 25, 2018